Loss of Outer Retinal Neurons and Circuitry Alterations in the DBA/2J Mouse

Laura Fernández-Sánchez,[1] Luis Pérez de Sevilla Müller,[2] Nicholas C. Brecha,[2–6] and Nicolás Cuenca[1]

[1]Department of Physiology, Genetics, and Microbiology, University of Alicante, San Vicente del Raspeig, Spain
[2]Department of Neurobiology, David Geffen School of Medicine, University of California at Los Angeles, Los Angeles, California, United States
[3]Department of Medicine, David Geffen School of Medicine, University of California at Los Angeles, Los Angeles, California, United States
[4]Jules Stein Eye Institute, David Geffen School of Medicine, University of California at Los Angeles, Los Angeles, California, United States
[5]CURE Digestive Diseases Research Center, David Geffen School of Medicine, University of California at Los Angeles, Los Angeles, California, United States
[6]U.S. Department of Veterans Affairs Greater Los Angeles Health System, Los Angeles, California, United States

Correspondence: Nicolás Cuenca, Department of Physiology, Genetics, and Microbiology, University of Alicante, San Vicente del Raspeig E-03690, Spain; cuenca@ua.es.

Submitted: March 22, 2014
Accepted: July 31, 2014

Citation: Fernández-Sánchez L, Pérez de Sevilla Müller L, Brecha NC, Cuenca N. Loss of outer retinal neurons and circuitry alterations in the DBA/2J mouse. *Invest Ophthalmol Vis Sci*. 2014;55:6059–6072. DOI:10.1167/iovs.14-14421

Purpose. The DBA/2J mouse line develops essential iris atrophy, pigment dispersion, and glaucomatous age-related changes, including an increase of IOP, optic nerve atrophy, and retinal ganglion cell (RGC) death. The aim of this study was to evaluate possible morphological changes in the outer retina of the DBA/2J mouse concomitant with disease progression and aging, based on the reduction of both the a- and b-waves and photopic flicker ERGs in this mouse line.

Methods. Vertically sectioned DBA/2J mice retinas were evaluated at 3, 8, and 16 months of age using photoreceptor, horizontal, and bipolar cell markers. Sixteen-month-old C57BL/6 mice retinas were used as controls.

Results. The DBA/2J mice had outer retinal degeneration at all ages, with the most severe degeneration in the oldest retinas. At 3 months of age, the number of photoreceptor cells and the thickness of the OPL were reduced. In addition, there was a loss of horizontal and ON-bipolar cell processes. At 8 months of age, RGC degeneration occurred in patches, and in the outer retina overlying these patches, cone morphology was impaired with a reduction in size as well as loss of outer segments and growth of horizontal and bipolar cell processes into the outer nuclear layer. At 16 months of age, connectivity between photoreceptors and horizontal and bipolar cell processes overlying these patches was lost.

Conclusions. Retinal degeneration in DBA/2J mice includes photoreceptor death, loss of bipolar and horizontal cell processes, and loss of synaptic contacts in an aging-dependent manner.

Key words: photoreceptor, horizontal cell, bipolar cell, synaptic triad, retinal degeneration, glaucoma.

Glaucoma is a heterogeneous group of chronic ocular diseases in which retinal ganglion cells (RGCs) die by apoptosis.[1,2] Glaucoma is the second most frequent cause of blindness in the world, representing 8% of all cases, according to the World Health Organization.[3] Angle-closure glaucoma usually develops an increase in IOP, leading to optic nerve damage, RGC death, and a permanent loss of vision.[2] The DBA/2J mouse line[4–6] has been suggested as a secondary angle-closure glaucoma model because of its close resemblance to this type of human glaucoma.[7] At 3 to 6 months of age, the DBA/2J mouse eye begins to develop essential iris atrophy, pigment dispersion, and glaucomatous age-related changes, including an increase of IOP, optic nerve atrophy, and RGC death. The DBA/2J mouse line carries recessive mutations in genes encoding glycosylated protein nmb (Gpnmb; NCBI GeneID 93695) and tyrosinase-related protein 1 (Tyrp1; NCBI GeneID 22178).[8,9] Mice with these mutations spontaneously develop iris atrophy, pigment deposition in the anterior segment, and eventually blockage of ocular drainage structures,[8] elevated IOP, optic nerve atrophy, and RGC degeneration, usually by apoptosis.[8,9] This ocular pathology may begin as early as 3 months of age.[10] Previous studies have evaluated and documented RGC degeneration and reduction of the inner retina concomitant with aging and disease progression in the DBA/2J mouse line.[10–12]

Electroretinograms (ERGs) performed on young DBA/2J mice (2–3 months) showed that both the oscillatory potentials and photopic flicker ERGs are lower than those from age-matched C57BL/6 mice,[13] whereas scotopic ERG responses had similar amplitudes in their a- and b-waves.[13,14] However, older DBA/2J mice (195–305 days) have lower amplitudes in their a- and b-waves compared with C57BL/6 mice.[13] Furthermore, a

TABLE. Primary Antibodies Used in This Work

Molecular Marker (Abbreviation)	Antibody(Reference)	Source and Catalog No.	Working Dilution
Bassoon	Mouse monoclonal[51]	Enzo Life Sciences, Plymouth Meeting, PA, USA (VAM-PS003)	1:1000
Calbindin D-28K (CB)	Rabbit polyclonal[48,60]	Swant, Bellinzona, Switzerland (CB-38a)	1:500
C-terminal binding protein-2 (CtBP2)	Mouse monoclonal, clone: 16/CtBP2[34]	BD Biosciences, San Diego, CA, USA (612044)	1:1000
Cytochrome C (Cyt C)	Mouse monoclonal, clone: 6H2.B4[61]	Zymed Laboratories, San Francisco, CA, USA (33-8200)	1:1000
Guanine nucleotide binding protein 3 (GNB3)	Rabbit polyclonal[31]	Sigma-Aldrich Corp., St. Louis, MO, USA (HPA005645)	1:50
Protein kinase C, α isoform (PKCα)	Rabbit polyclonal[60]	Santa Cruz Biotechnology, Santa Cruz, CA, USA (sc-10800)	1:100
Synaptophysin (SYP)	Mouse monoclonal, clone: SY38[60,19]	Chemicon-Millipore, Temecula, CA, USA (MAB5258)	1:1000
Syntaxin 4 (STX4)	Rabbit polyclonal[36]	Chemicon-Millipore (AB5330)	1:500
Transducin, Gαc subunit (Gt)	Rabbit polyclonal[62,60]	Cytosignal, Irvine, CA, USA (PAB-00801-G)	1:200
Vesicular glutamate transporter 1 (VGLUT1)	Guinea Pig polyclonal[36]	Chemicon (AB5905)	1:1000
Brain-specific homeobox/POU domain protein 3A (Brn-3a)	Goat polyclonal	Santa Cruz Biotechnology (sc-31984 L)	1:500

significant reduction of the scotopic a- and b-wave amplitudes has also been reported for 2-year-old DBA/2J mice,[15] suggesting changes in the functional integrity of the outer retina, as these waves are mainly generated by photoreceptor and ON bipolar cell responses.[16,17] Fuchs et al.[18] found a narrowing of the outer plexiform layer (OPL) that they attribute to structural synaptic ribbon impairment in the axon terminal of rod photoreceptors. However, there is poor information available regarding cellular or synaptic changes in the outer retina of the DBA/2J line with aging and disease progression that could account for these changes in the ERG. In this study, we have evaluated the cellular morphology of the outer nuclear layer (ONL) and the organization of the OPL of the DBA/2J mouse retina at different ages, before and after the onset of RGC degeneration.

MATERIALS AND METHODS

Animals and Tissue Preparation

Female DBA/2J (*Gpnmb*^{R150X} and *Tyrp1*^{isa}) mice at 3, 8, and 16 months of age, with a total of 12 animals, were used in this study. Female C57BL/6 mice at 16 months of age were used as controls. Animals were obtained from the Jackson Laboratory (Bar Harbor, ME, USA). They were maintained and bred in temperature- and light-controlled rooms with a 12-hour light/dark cycle and had food and water ad libitum at the David Geffen School of Medicine at the University of California, Los Angeles (UCLA). DBA/2J is a well-studied secondary angle-closure glaucoma model presenting IOP increase. The IOP measurements reported by others and us showed increased IOP in this model starting at approximately 6 months old and is maintained with aging.[4,12] All experiments were performed in accordance with the guidelines and policies for the welfare of experimental animals established by the US Public Health Service Policy on Human Care and Use of Laboratory Animals (2002), the UCLA Animal Research Committee, and the ARVO Statement for the Use of Animals in Ophthalmic and Vision Research. The mice were deeply anesthetized with 1% to 3% isofluorane (Novaplus, Lake Forest, IL, USA). The eyes were enucleated and fixed in cold 4% paraformaldehyde in 0.1 M PBS, pH 7.4, for 60 minutes at room temperature (RT). Eyes were immersed in 15% and then 20% sucrose in PBS for 1 hour each, and left in 30% sucrose in PBS overnight at 4°C. The following day, the cornea, lens, and vitreous body were removed and embedded in Tissue-Tek OCT (Sakura Finetek, Zoeterwouden, The Netherlands) and frozen in liquid N_2. Vertical sections of the retina were cut at 16-μm thickness on a cryostat (Leica CM 1900; Leica Microsystems, Wetzlar, Germany) in a horizontal plane, and mounted on Superfrost Plus slides (Menzel GmbH & Co KG, Braunschweig, Germany), and air-dried.

Immunohistochemistry

For immunohistochemistry, at least three animals were studied at each time point. Retinas from C57BL/6 and DBA/2J mice were processed in parallel, and retinal sections were treated as in previous studies.[19–22] Briefly, the sections were thawed and washed three times for 10 minutes in 0.1 M phosphate buffer (PB), pH 7.4, and then incubated in blocking solution (10% normal donkey serum in 0.1 M PB containing 0.5% Triton X-100) for 1 hour at RT in the dark. The sections were then incubated in the primary antibodies diluted in PB containing 0.5% Triton X-100 overnight at RT. All primary antibodies used in this work (summarized in the Table) had been used in several previous studies and are well characterized by others and us regarding cell type specificity. The sections were subsequently washed in PB and incubated in the corresponding secondary antibodies at a 1:100 dilution for 1 hour at RT. Secondary antibodies used in this work were AlexaFluor 488–anti-rabbit IgG, AlexaFluor 555–anti-mouse IgG donkey, and AlexaFluor 633–anti-guinea pig IgG donkey (Invitrogen, Carlsbad, CA, USA). The nuclear marker, TO-PRO-3 iodide (Invitrogen) was added at 1 μM with the secondary antibodies. The sections were finally washed three times for 10 minutes in PB, mounted in Citifluor (Citifluor Ltd., London, UK) and cover-slipped for viewing with a Leica TCS SP2 laser-scanning confocal microscope. To control for nonspecific staining, some sections were processed without the primary antibody. Final images from C57BL/6 and DBA/2J retinas were processed in parallel using the Adobe Photoshop 10 software (Adobe Systems, Inc., San Jose, CA, USA).

Morphometric Analysis

Measurements of the ONL were performed on retinal sections stained with TO-PRO 3-iodide. Sections stained with antibodies against calbindin at different ages were used to quantify the

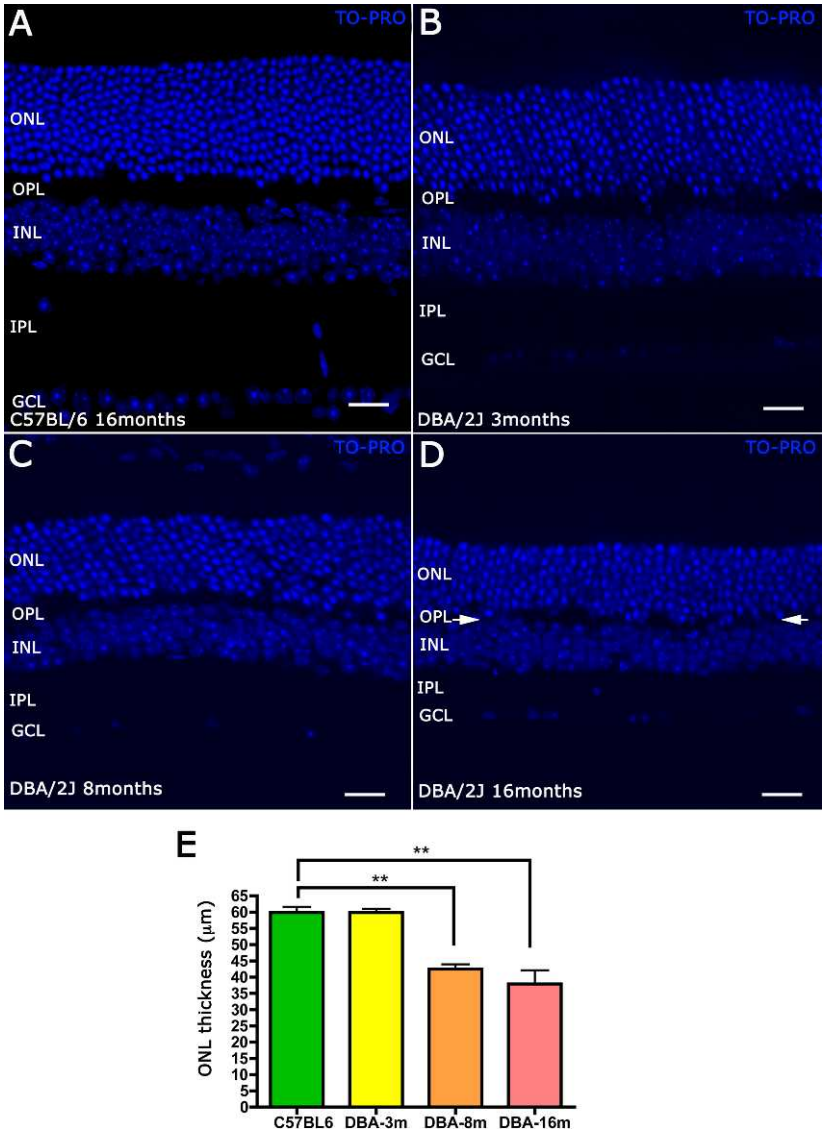

Figure 1. Vertical sections from C57BL/6J retina at 16 months (**A**), and DBA/2J retina at 3, 8, and 16 months (**B**–**D**). Immunostained with the nuclear marker TO-PRO 3-iodide showed a reduction in the number of cellular rows in the ONL and INL and a reduction in cell bodies in the GCL, likely corresponding to RGCs. The quantification is shown in (**E**) (**$P < 0.01$). *Scale bars*: 20 μm.

invaginated terminal tips of horizontal cells into the photoreceptor axon terminals. All measurements were taken in the central area, near the optic nerve head, of at least three animals in eight single-scanned pictures at each eye and age point. At 8 and 16 months, digital images were taken inside and outside the patches. The patches in retinal sections were defined as areas with greater loss of photoreceptor cells, decreased synaptic connectivity in the OPL, with high diminution in the horizontal cell plexus. In addition, it was possible to find inside these areas vascular alterations in the superficial plexus together with retinal remodelation (Supplementary Material S1). ImageJ software (http://imagej.nih.gov/ij/; provided in the public domain by the National Institutes of Health, Bethesda, MD, USA) was used for the morphometric analysis of the confocal images; the quantification of horizontal cell tips was done manually using the cell counter plugin.

Statistical Analyses

Results were analyzed by Graphpad Prism (GraphPad Software, Inc., La Jolla, CA, USA). For statistical analysis, two-tailed Student's *t*-test was performed to compare the ONL thickness and the number of horizontal cell tips found at each age-point compared with control retina. *P* values of less than 0.05 were considered to be statistically significant.

Results

Retinal Thickness in the DBA/2J Mice

The thickness of the ONLs and inner nuclear layers (INLs) was evaluated using a nuclear stain, TO-PRO 3-iodide. Measurements were made on vertical sections of central retina, 100 μm from the optic nerve head. In vertical sections of 16-month-old C57BL/6 retinas, the ONL consisted of 12 to 14 rows of photoreceptor cell bodies, the INL consisted of five rows of cell bodies, and there was a regular distribution of cells, including RGCs in the ganglion cell layer (GCL) (Fig. 1A). In 3-month-old DBA/2J retinas, the thickness of both nuclear layers appeared normal compared with C57BL/6 retinas, although there were some subtle alterations in the OPL, including

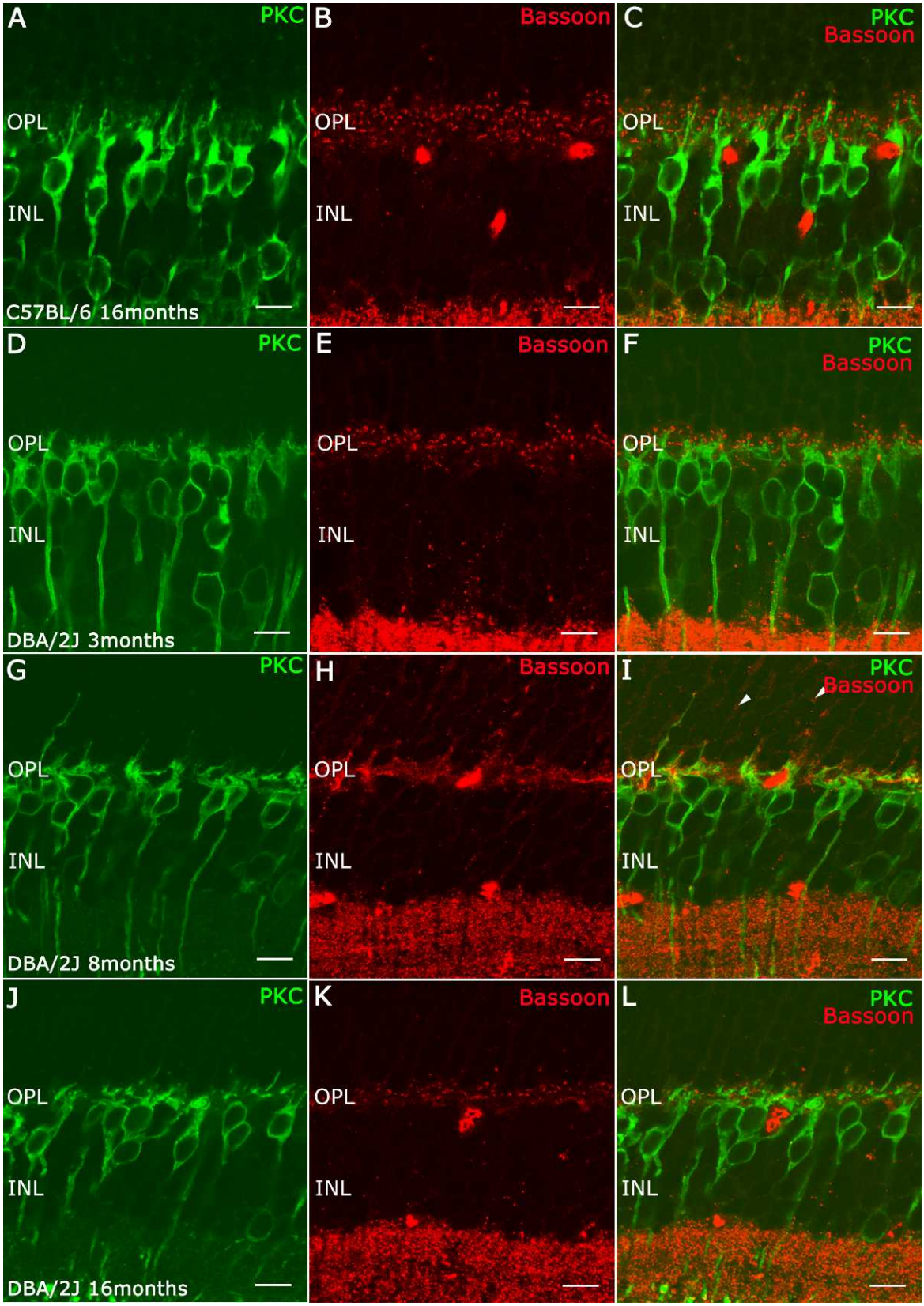

Figure 2. Immunolabeling for α-PKC (*green*) and Bassoon (*red*) on vertical sections. (**A–C**) Retina of C57BL/6J mice at 16 months of age. Retinal of DBA/2J mice at 3 months (**D–F**), 8 months (**G–I**), and 16 months (**J–L**). (**A**, **D**, **G**, **J**) Immunolabeling for α-PKC showing loss of dendrites of rod bipolar cells in the DBA/2J retina in older animals. (**B**, **E**, **H**, **K**) Immunolabeling for Bassoon showing the diminution of synaptic ribbons in the OPL in this animal model. (**C**, **L**, **F**, **I**) Merge. *Scale bars*: 10 μm.

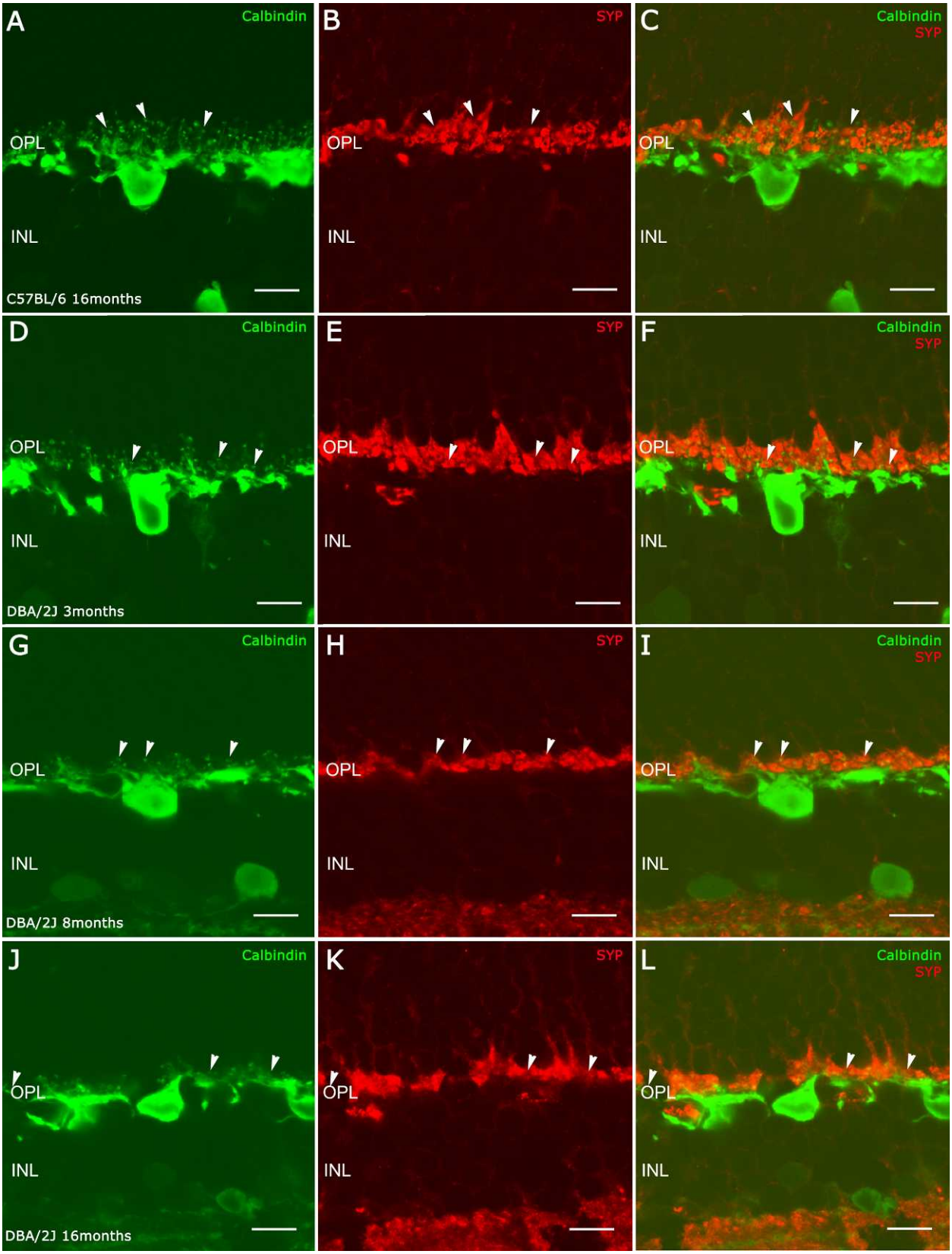

Figure 3. Cryostat sections of C57BL/6J (**A**–C) and DBA/2J retinas at 3 months (**D**–**F**), 8 months (**G**–**I**), and 16 months (**J**–**L**). Immunolabeling for calbindin ([**A**, **D**, **G**, **J**] *arrowheads*) showing the loss of terminal tips of horizontal cells in the DBA/2J retina. Immunolabeling for synaptophysin (**B**, **E**, **H**, **K**) showing the diminution of the photoreceptor axon terminals. (**C**, **L**, **F**, **I**) Merge. *Scale bars*: 10 μm.

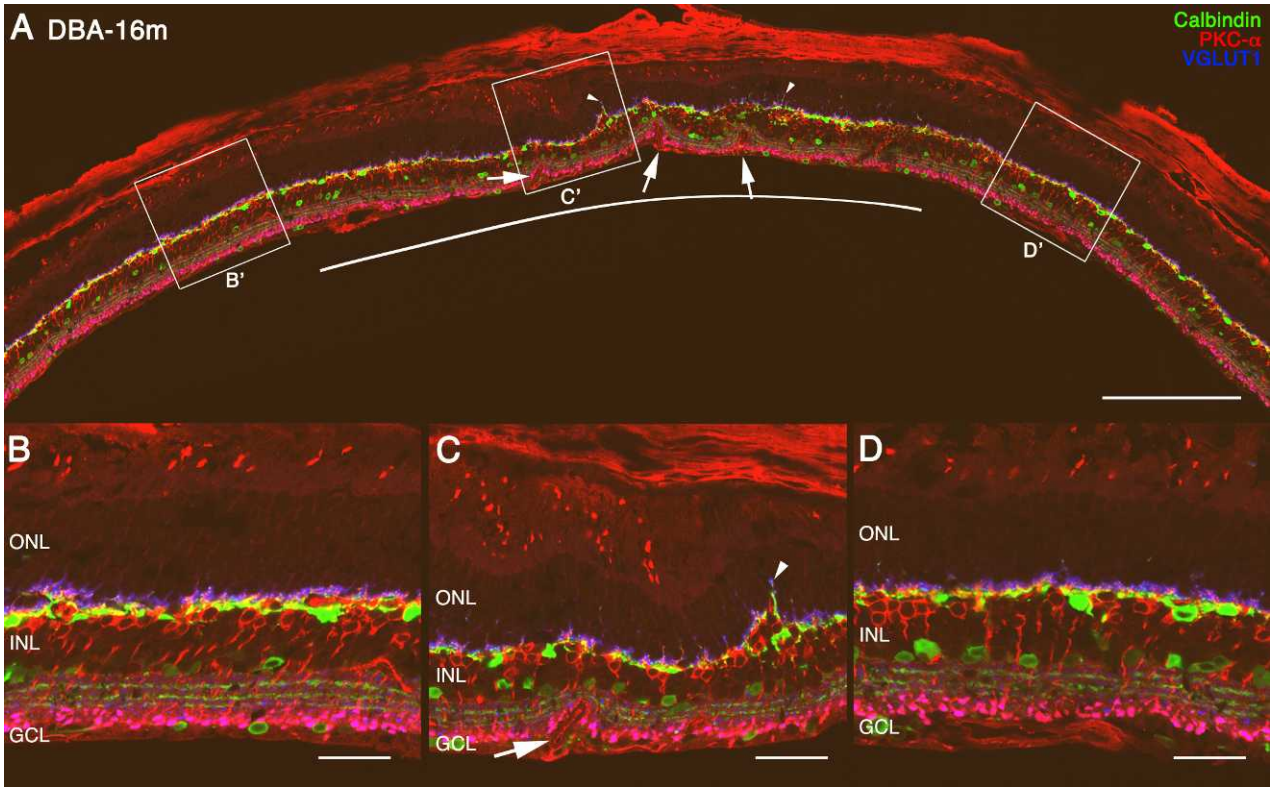

FIGURE 4. Low-magnification cross section of retinas labeled with antibodies against α-PKC (*red*), calbindin (*green*), and VGLUT1 (*blue*). Retina of DBA/2J mice at 16 months old (**A**) showing a panoramic view of a retinal patch (*area underlying white line*). In high magnification of this area ([**C**] high magnification from [**C'**]), the loss of photoreceptor cells, sprouting of bipolar and horizontal cells into the ONL (*arrowheads*), loss of horizontal plexus in the OPL, and vascular alterations (*arrows*) can be observed compared with areas outside patches ([**B**, **D**] high magnification from [**B'**] and [**D'**] in [**A**], respectively). *Scale bars*: 200 μm (**A**); 40 μm (**B–D**).

misplaced nuclei resulting in discontinuities in the thickness of the OPL (Fig. 1B). These observations in the OPL at 3 months are consistent with findings from a previous report.[18] At 8 months old, the ONL was reduced to 9 to 11 rows of photoreceptor cell bodies and the INL was approximately 4 cellular rows (Fig. 1C). Quantification of ONL thickness showed a statistically significant reduction of approximately 20 μm in DBA/2J mice compared with C57BL/6, which can be converted in the loss of approximately three to four photoreceptor rows (Fig. 1E). The width of the OPL and inner plexiform layer (IPL), at this age, was noticeably thinner than the OPL and IPL in the control retinas, and there was a marked reduction in cell number in the GCL (Fig. 1C). At 16 months of age, DBA/2J mice displayed a high variability between different animals in the ONL thickness. We found a reduction of six to seven rows of photoreceptor cell bodies, the quantification showed a statistically significant reduction compared with C57BL/6 retinas (Fig. 1E). Furthermore, the reduction in the OPL and IPL thickness was evident, and in some areas, the OPL was difficult to identify (Fig. 1D, arrows).

Alterations in the Connectivity at the OPL Level

The photoreceptor synaptic triad[23–25] consists of a rod or cone axon terminal characterized by a synaptic ribbon, and two horizontal processes and a bipolar dendrite that invaginate the axonal terminal.

Connectivity Between Photoreceptor and Rod Bipolar Cells. To evaluate the distribution of rod bipolar cell dendrites in rod synaptic triads, we performed double-label immunostaining using antibodies against protein kinase C (PKC)-α, for rod bipolar cells, and Bassoon, a marker of the arciform density underlying the synaptic ribbon[26] (Fig. 2). In C57BL/6 retinas at 16 months old (Figs. 2A–C), the outer retina appeared to have a normal morphology, with bipolar cell dendrites terminating near Bassoon immunoreactive puncta, which demark the photoreceptor synaptic ribbon (Figs. 2A–C). In 3-month-old DBA/2J retinas (Figs. 2D–F), the rod bipolar cell dendrites (Fig. 2D, green) were retracted with shorter tips compared with bipolar cells in C57/Bl retinas, and there was a significant decrease of Bassoon immunoreactive puncta (Fig. 2E, red). These anatomical changes are more apparent at older ages. In 8-month-old DBA/2J retinas (Figs. 3G–I), most rod bipolar cells lacked dendrites, although there were a few dendrites that extended into the ONL (Fig. 2G). In addition, there were few Bassoon immunostained puncta (Fig. 2H) compared with earlier ages, and some of these puncta were not associated with bipolar dendrites (Fig. 2I, arrowhead), whereas other Bassoon immunoreactive puncta were localized at the end of dendrites in the ONL (Fig. 2I, arrow), indicative of a retraction of the rod spherules. In 16-month-old DBA/2J retinas, only a few bipolar cell dendrites remained (Fig. 2J) and there was an overall reduction of Bassoon immunoreactive puncta (Figs. 2K, 2L).

Connectivity Between Photoreceptors and Horizontal Cells. To identify horizontal cell axons and dendrites, we used an antibody to calbindin[27] (Figs. 3A, 3C). Photoreceptor axonal terminals were identified using an antibody to synaptophysin, a protein associated with synaptic vesicles[28] (Figs. 3B, 3C).

The C57BL/6 retinas at 16 months old showed a regular distribution of horizontal cell dendritic tips and synaptophysin staining in rod and cone photoreceptor axon terminals

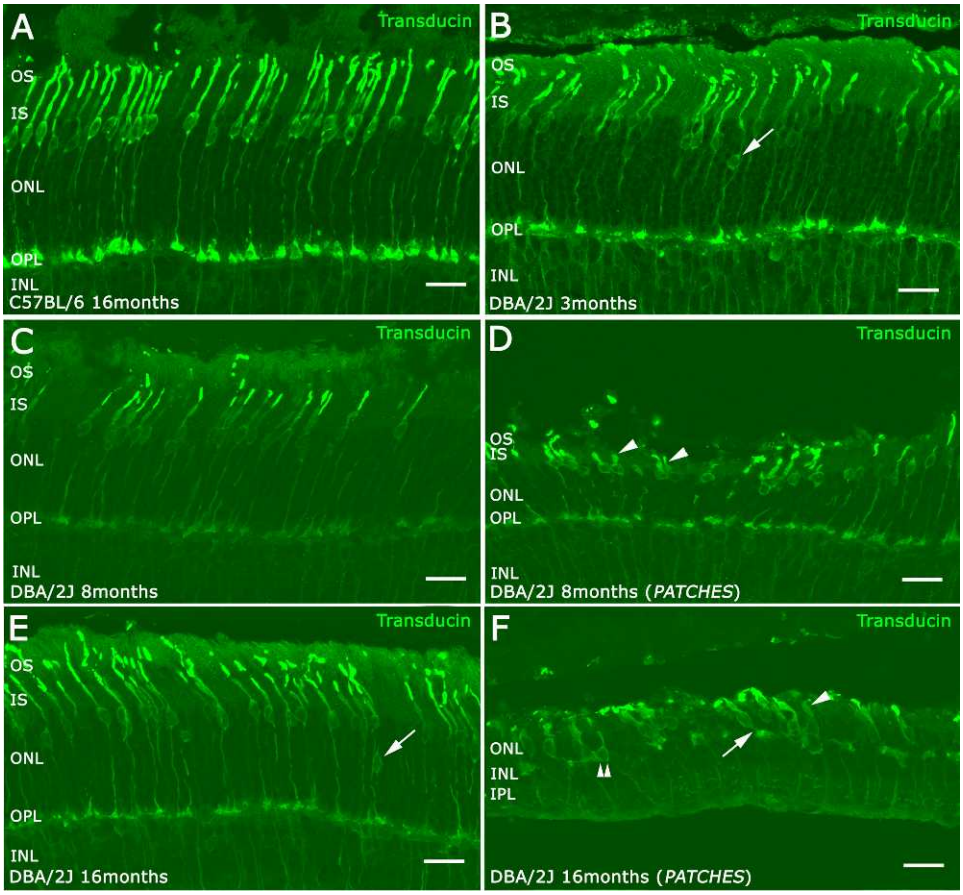

Figure 5. Retinal morphology of cone photoreceptor. γ-Transducin antibodies were used to visualize cone morphology in vertical retina sections of C57BL/6 retinas (**A**), DBA/2J retinas at 3 months (**B**), 8 months (**C**, **D**) and 16 months (**E**, **F**). The nuclei of cone photoreceptors showed an abnormal localization at the ONL level at 3 months ([**B**] *arrow*) and at 16 months ([**E**] *arrow*). Inside the patches (**D**, **F**) the IS of cones were swollen (*arrowheads*) and had short axons or absent (*double arrowheads*). *Scale bars*: 20 μm.

associated with horizontal cell endings (Figs. 3A–C). In 3-month-old DBA/2J retinas (Figs. 3D–F), there was a shortening of horizontal cell processes and a clear reduction of horizontal cell endings (Fig. 3D, arrowheads) compared with C57BL/6 retinas (Fig. 3A, arrowheads), although the expression of synaptophysin immunostaining in the photoreceptor axon terminals (Fig. 3E) appears to remain at the same level as control retinas (Fig. 3B). In 8-month-old DBA/2J retinas (Figs. 3G–I), the loss of horizontal cell processes and tips was more apparent (Figs. 3G, 3I, arrowheads) compared with control retinas (Fig. 3A, arrowheads). The staining of photoreceptor axon terminals with synaptophysin showed only one to two rows at the OPL at this age (Figs. 3H, 3I). In 16-month-old DBA/2J retinas (Figs. 3J–L), there was a discontinuous plexus of horizontal cell processes in the OPL with few endings (Figs. 3J, 3L), as well as a reduction of the photoreceptor axon terminals (Figs. 3H, 3K).

Degeneration in Retinal "Patches"

At 6 to 8 months of age in the DBA/2J retina, degeneration and loss of cells in the GCL is apparent[4,10,11] and located in discontinuous retinal areas.[29] Over time, these areas of RGC loss expand to cover most of the retina (see Supplementary Materials S2).

In retinal sections, we identified areas with changes in the inner and outer retina, which were referred to as "patches" compared with other areas in the same retinal section (Fig. 4). These patches (Fig. 4C) are areas where photoreceptors are lost and the OPL and INL present alterations with a substantial decrease in the horizontal cell plexus (see Supplementary Materials S1) and increased retraction of photoreceptor cell axons accompanied by sprouting of horizontal and bipolar cells (Figs. 4A, 4C, arrowheads). Inside these areas it is possible to find vascular alterations (Figs. 4A, 4C, arrows) compared with neighbor areas with normal appearance (Figs. 4B, 4D).

Cone Photoreceptors. To evaluate cone photoreceptor morphology, retinal sections were immunostained with an antibody against γ-transducin, a specific marker for cone photoreceptors.[30] To avoid the differences in cone density in different areas of the retina, the photographs for cone morphology studies were taken in the temporal area near optic nerve and inside the patches in all animals. The morphology of cone photoreceptors was well preserved in the DBA/2J retina at 3 (Fig. 5B), 8, and 16 months of age outside of the patches (Figs. 5C, 5E). In C57BL/6 retina at 16 months of age, the nuclei of cone photoreceptor cells were located in the distal ONL (Fig. 5A). In the DBA/2J retina at 3 months of age, some cone nuclei were located in the middle of the ONL (Fig. 5B, arrows). At 8 months of age, there were patches with a greater degeneration compared with other areas of the retina. There was a marked loss of rows of photoreceptor cell bodies in the ONL in these regions. Cone photoreceptor morphology was altered, with an overall reduction in length, shorter outer segments (OS) and swollen inner segments (IS) (Fig. 5D, arrowheads). At 16 months of age,

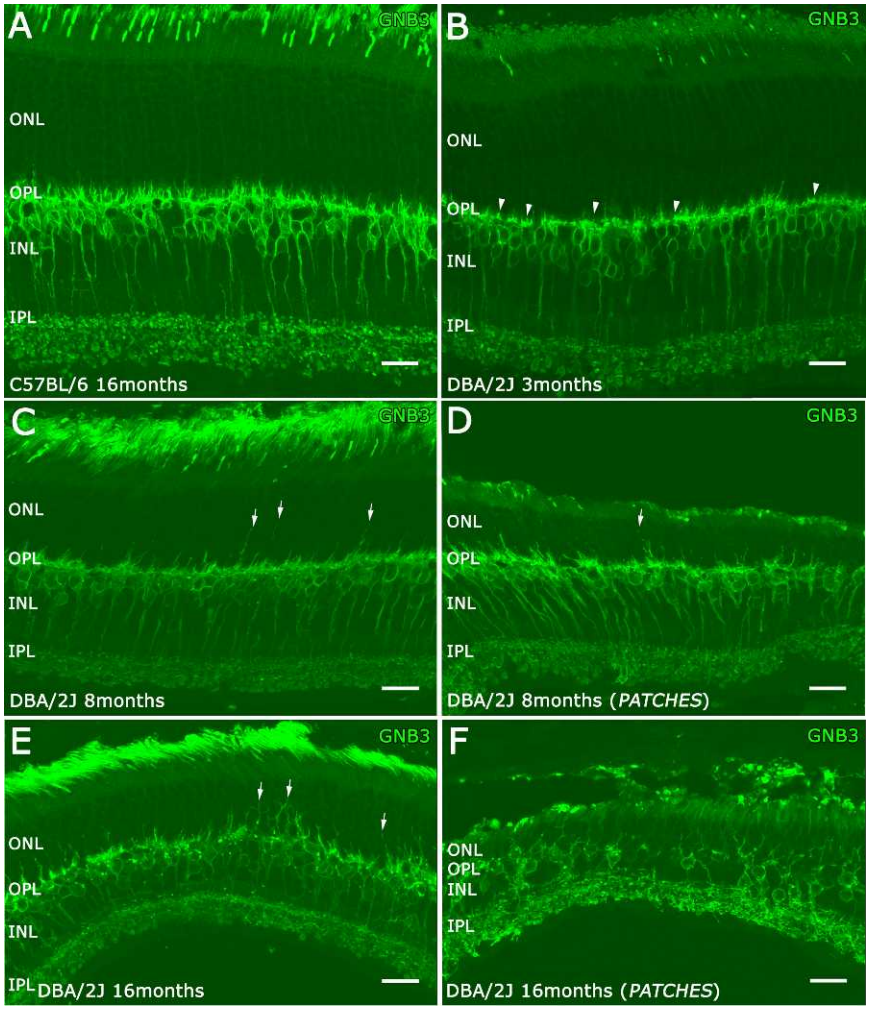

Figure 6. Bipolar cells immunostained with GNB3 antibodies. The GNB3 staining showed retraction of bipolar dendrites at 3 months old in the DBA/2J retina ([**B**] *arrowheads*) compared with C57BL/6 retina (**A**). The DBA/2J retinas have bipolar cell dendritic growth at 8 months (**C**, **D**, *arrows*) until 16 months of age ([**E**] *arrows*; [**F**]). This dendritic growth was more evident inside the patches (**D**, **F**). *Scale bars*: 20 μm.

cone morphology was markedly impaired (Fig. 5F) compared with outer retinal regions that overlay retinal regions with RGCs (Fig. 5E). At this age, most cone photoreceptor cells lacked an obvious axon terminal (Fig. 5F, double arrowhead) and only a few cone photoreceptor cells were observed having a short axonal terminal (Fig. 5F, arrows). In addition, the cone IS were swollen (arrowheads) and the OS were quite small (Fig. 5F), compared with control retinas (Fig. 5E).

Bipolar Cells. Guanine nucleotide-binding protein β3 (GNB3), an isoform of the β subunit of a G-protein commonly associated with transmembrane receptors, is expressed by cone photoreceptors, and ON cone and ON rod bipolar cells.[31] Therefore, we used an antibody against GNB3 to evaluate bipolar cell morphology in the C57BL/6 and DBA/2J retinas (Fig. 6). In 3-month-old DBA/2J retinas, GNB3 immunostaining showed a slight reduction of the bipolar cell dendrites (Fig. 6B, arrowheads) and the bipolar axon terminals in the IPL appeared to be less frequent and swollen compared with bipolar cells in C57BL/6 (Fig. 6A). In 8-month-old DBA/2J retinas, a few GNB3 immunostained bipolar cell dendrites were present in middle of the ONL (Figs. 6C, 6D, arrows). The IPL was thinner at this age, and there were fewer bipolar cell axon terminals that were smaller than the bipolar cell axonal terminals in the C57BL/6 retina. In 16-month-old DBA/2J retinas, a greater number of bipolar cell dendrites showed growth into the ONL (Fig. 6E, arrows). In addition, at this age, bipolar cell bodies were disorganized in the INL, and there was a loss of axonal terminals and lateral varicosities in the IPL, especially over regions of RGC loss (Fig. 6F).

Synaptic Connectivity Between Photoreceptor and Horizontal Cells. To evaluate alterations in the synaptic connectivity between photoreceptors and horizontal cells in the OPL, we performed triple immunostaining studies using markers for photoreceptor axonal terminals, the photoreceptor synaptic ribbon, and horizontal cell processes. Antibodies against the vesicular glutamate transporter type 1 (VGLUT1), which transports glutamate into synaptic vesicles,[32] was used to visualize cone and rod axon terminals. To identify the synaptic ribbon in the photoreceptor axon terminal, antibodies were used to detect the C-terminal binding protein 2 (CtBP2), which is domain B of RIBEYE, a structural protein of synaptic ribbons.[33–35] Antibodies to calbindin were used to visualize horizontal cell processes (Fig. 7). In the C57BL/6 retina (Fig. 7A), VGLUT1 immunostaining showed three to four rows of rod spherules in the OPL, and each rod spherule contained a synaptic ribbon, identified by CtBP2 immunoreactive puncta adjacent to the tip of the horizontal cell ending (Fig. 7A). In 3-month-old DBA/2J retinas (Fig. 7B), there was a small reduction in the thickness of the OPL compared with the C57BL/6 retinas (Fig. 7A). The quantification of the number of horizontal cell

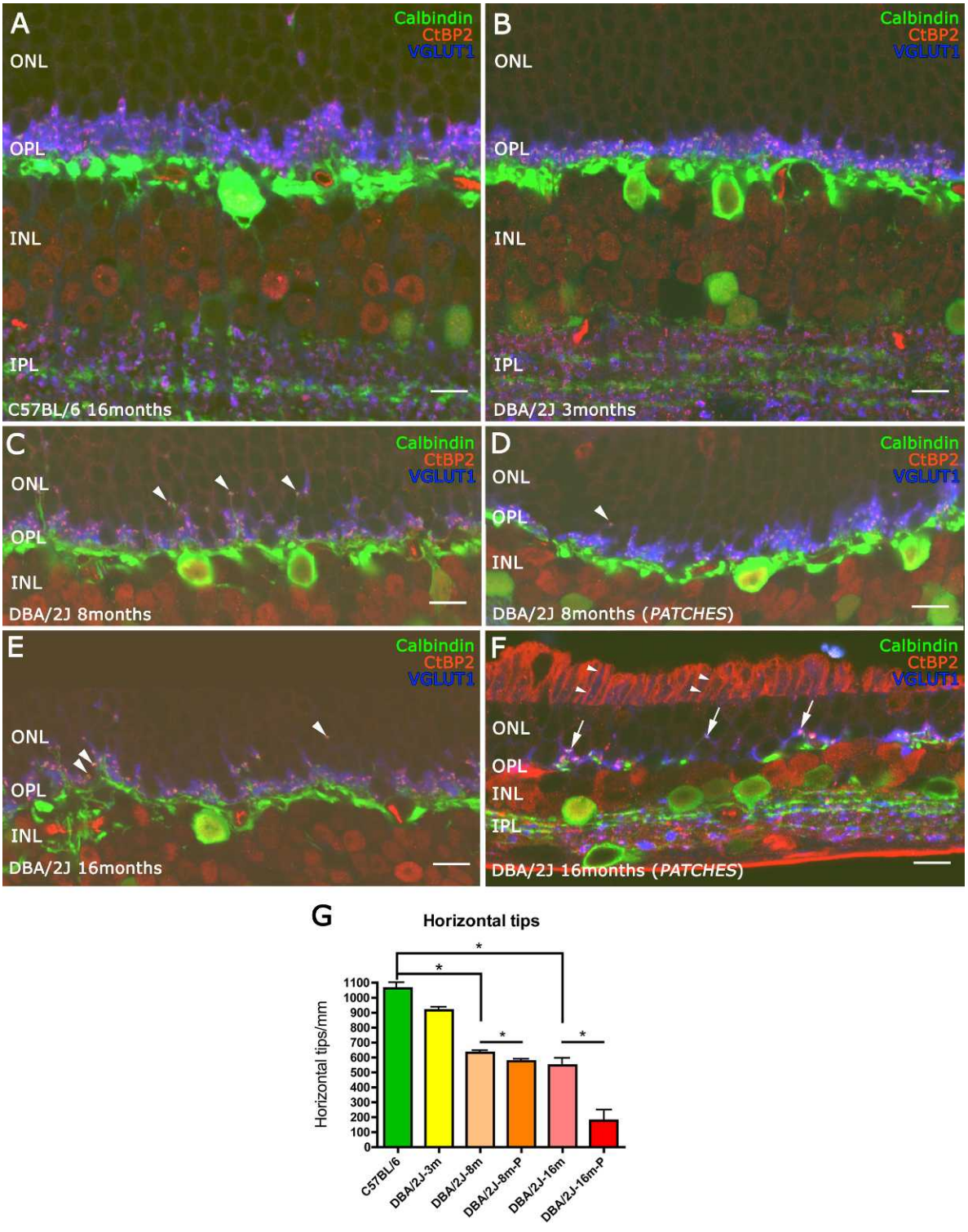

Figure 7. Three specific markers of synaptic structure were used to study the connectivity between photoreceptor and horizontal cells. Antibodies against CtBP2 (*red*) and VGLUT1 (*blue*) were used to visualize the axon terminal structures of photoreceptor cells, and calbindin (*green*) was used to visualize horizontal cell dendrites. A thinning in the OPL was observed at 3 months old in the DBA/2J retinas (**B**) compared with C57BL/6 retinas (**A**). From 8 months (**C**, **D**) to 16 months (**E**, **F**), DBA/2J retinas showed growth of horizontal cells and synaptic contacts without VGLUT1 immunoreactivity (*arrowheads*). At 16 months old, inside the patches, only some synaptic contacts were complete ([**F**] *arrows*) and the plexus of the horizontal cells at OPL level were nearly absent. Quantification of horizontal cell terminal tips is shown in (**G**). $^*P < 0.05$. *Scale bars*: 10 μm.

showed a reduction of 10% compared with C57BL/6 retinas (Fig. 7G). In 8- and 16-month-old DBA/2J retinas, the loss of connectivity between photoreceptors and horizontal cell endings was evident (Figs. 7C, 7E). There was a loss of approximately 40% and 48% of the horizontal cell tips at 8 and 16 months, respectively, over the retinal regions with RGCs (Fig. 7G). In contrast, in outer retinal regions overlying regions of RGC loss ("patches"), at 16 months the decrease in the

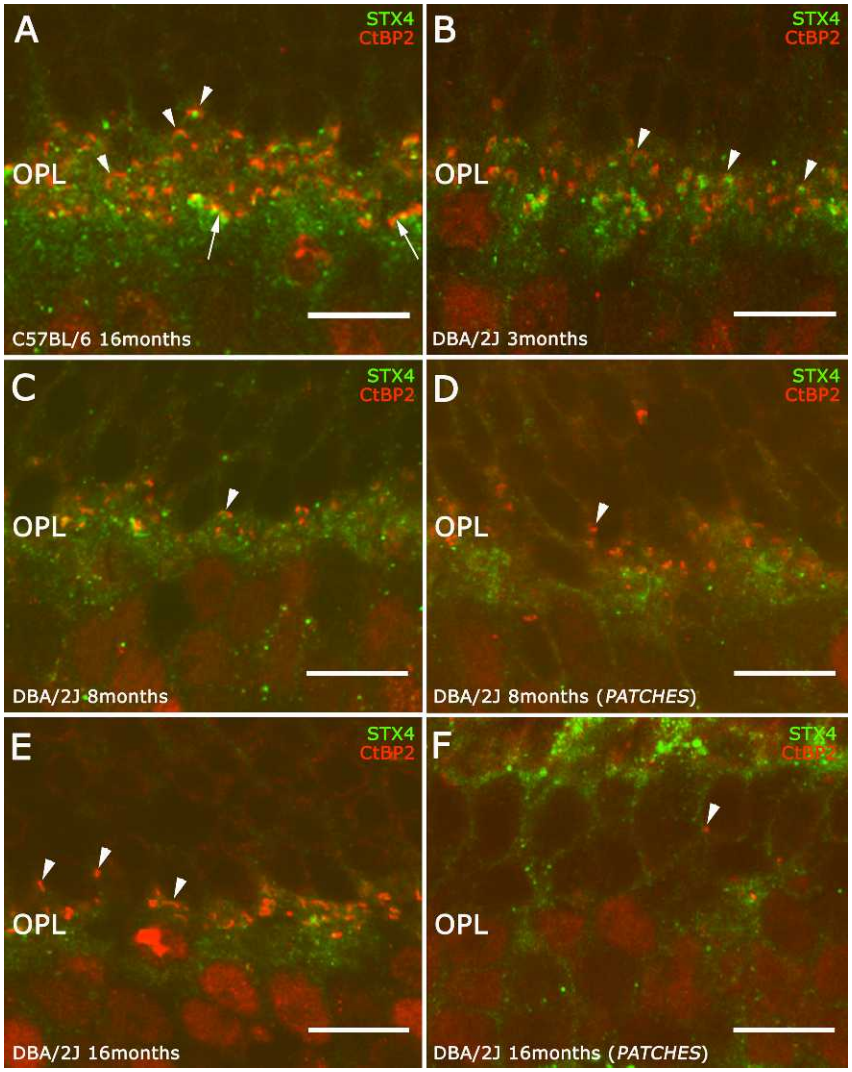

Figure 8. Study of connectivity lost between photoreceptor and horizontal cells. A double immunostaining against syntaxin 4 (*green*) and CtBP2 (*red*) was used to evaluate the loss of photoreceptor and horizontal contacts. In the C57BL/6 retinas (**A**) and in DBA/2J retinas at 3 months old (**B**), each point of CtBP2 had the corresponding syntaxin 4 (STX4) spot. This relation was disrupted from 8 months old inside the patches (**D**, *arrowheads*) to 16 months old in the DBA/2J retinas ([**E**, **F**], *arrowheads*). There was a reduction in the contacts at 8 months old in the DBA/2J retinas. *Scale bars*: 10 μm.

number of horizontal cell tips was approximately 80% (Fig. 7G), and only a very few horizontal cell tips, axonal terminals, and photoreceptor ribbons were identified (Fig. 7F). In addition, at 8 and 16 months, overlying regions where RGCs remain, a few horizontal cell tips were observed in the ONL, indicating growth into the photoreceptor nuclear layer (Figs. 7C, 7E). No VGLUT1 immunoreactivity was present in the axon terminals (Figs. 7C, 7E, arrowheads), although the pairs between horizontal cell tips (calbindin, green) and photoreceptor ribbons (CtBP2, red) were still present.

Similar findings were observed at 8 months inside the patches (Fig. 7D). At 16 months of age, no horizontal cell bodies were found in regions above the "patches" and there was a corresponding loss of the horizontal cell plexus in the OPL. In these regions, a reduction of calbindin and CtBP2 immunoreactive puncta was evident (Fig. 7F, arrows). In addition, CtBP2 and VGLUT1 immunoreactivity was found in the inner and outer segments of the photoreceptors (Fig. 7F, arrowheads), instead of in the photoreceptor axon terminal.

To determine if horizontal cell processes are in apposition to photoreceptor terminals near the synaptic ribbon, and verify whether postsynaptic contacts with horizontal cells were lost, we performed double-label immunostaining with antibodies against CtBP2 (Fig. 8, red), and against syntaxin 4 (Fig. 8, green), a marker of horizontal cell tips.[36] The typical horseshoe morphology corresponding to photoreceptor ribbons in rod spherules is associated with horizontal cell tips (Fig. 8A, arrowheads) and the disk-like morphology corresponding to photoreceptor ribbons in cone pedicles is also associated with horizontal cell dendrites (Fig. 8A, arrows).

In 3-month-old DBA/2J retinas (Fig. 8B), there was a clear decrease of photoreceptor ribbons together with a loss of their horseshoe morphology compared with C57BL/6 retinas (Fig. 8A). Some of the CtBP2 puncta observed were lacking their corresponding syntaxin 4 immunoreactive spot (Fig. 8B, arrowheads). In 8-month-old DBA/2J retinas, there was a reduction of the CtBP2 and syntaxin 4 pairs. In addition, the horseshoe morphology of the ribbon changed to a small immunoreactive puncta and pairs of CtBP2 and syntaxin 4

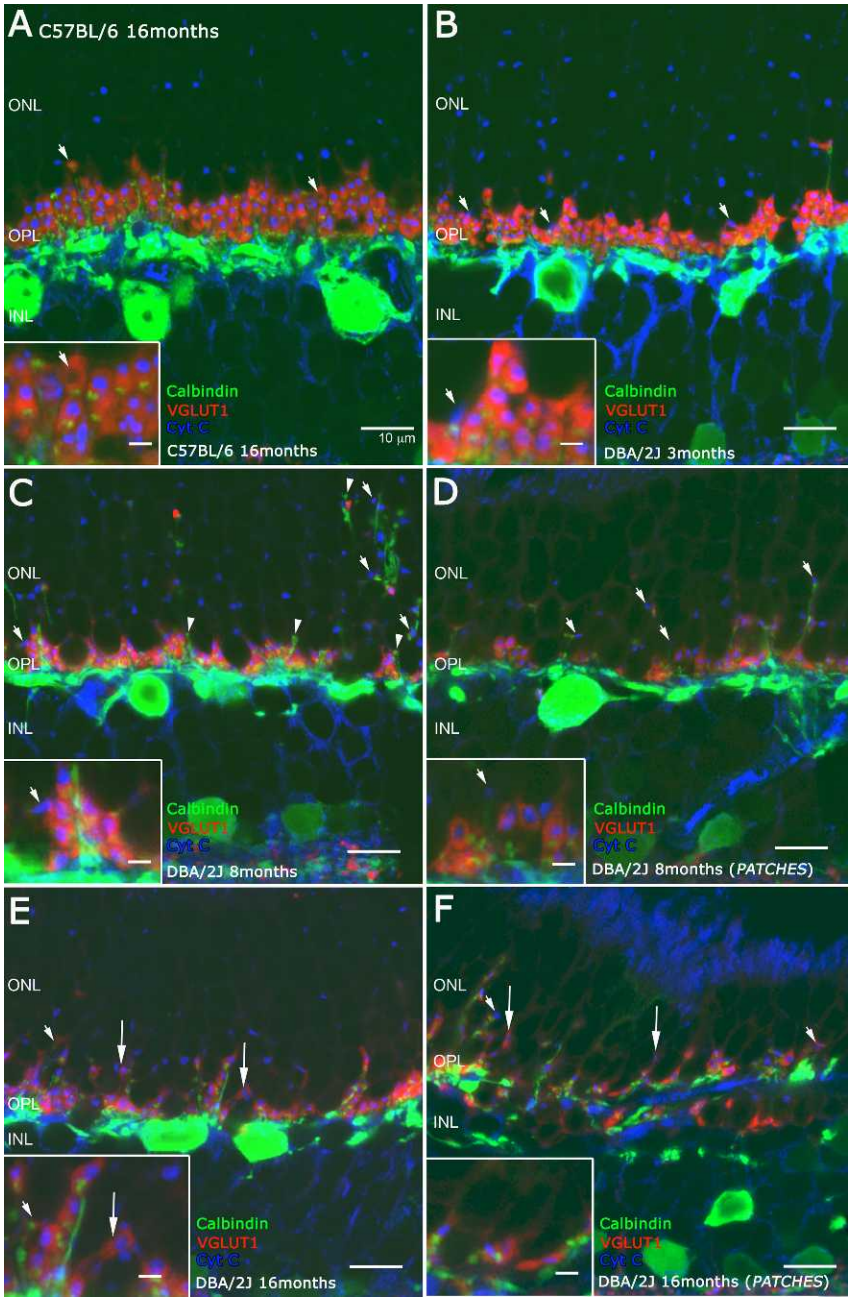

Figure 9. Vertical sections of retinas stained with antibodies against calbindin (*green*) to visualize horizontal dendrite tips, VGLUT1 (*red*) for photoreceptor axon terminals staining, and Cyt C (*blue*) to visualize the giant mitochondria. The panel shows normal connections between photoreceptor and horizontal cells in C57BL/6 retinas at 16 months (**A**) compared with the connections of DBA/2J retinas at 3 months where some photoreceptor axons have lost VGLUT1 staining ([**B**] *arrows*). At 8 months (**C**, **D**), DBA/2J retinas show growth of horizontal cell processes outside the patches ([**C**] *arrows*) and loss of contacts with photoreceptor axons and horizontal tip retraction ([**C**] *arrowheads*). The DBA/2J retinas at 16 months of age have some axon terminals adjacent to horizontal cell processes both outside and inside the patches ([**E**, **F**] *arrows*). *Scale bars*: 10 µm. *Scale bars in the high magnification*: 2 µm.

immunoreactive puncta were rare (Fig. 8C, arrowheads). These changes were more evident in outer retinal regions above the patches of RGC loss (Fig. 8D, arrowheads). The impairment of synaptic contacts was more evident at 16 months of age (Fig. 8E), where there were many examples of CtBP2 immunoreactive puncta without a corresponding syntaxin 4 immunoreactive puncta (Fig. 8E, arrowheads). In outer retinal regions over the patches lacking RGCs at 16 months old, the pairs CtBP2 and syntaxin 4 in the OPL were infrequent. Only sporadic pairs can be recognized (Fig. 8F, arrow). Some CtBP2 puncta were located in the ONL and were not associated with syntaxin 4 immunoreactivity (Fig. 8F, arrowhead).

Photoreceptor Axon Terminal Morphology. Neurotransmitter release requires ATP for synaptic vesicle release, which is generated by large mitochondrion in the rod photoreceptor terminals.[33,37–39] To study the energetic conditions of the photoreceptor axon terminals, we used antibodies against cytochrome C (Cyt C) as a marker of mitochondrion. The VGLUT1 and calbindin antibodies were used to visualize rod spherules and cone pedicles, and horizontal cell endings, respectively. In the C57BL/6J mouse retina at 16 months of age,

rod spherules express VGLUT1 immunoreactivity, and the horizontal endings in the synaptic triad can be easily recognized (Fig. 9A, inset, arrow). The giant mitochondrion expressing Cyt C immunoreactivity (Fig. 9, blue) was also visualized in the rod spherules.[39] In 3-month-old DBA/2J retinas, VGLUT1 immunoreactivity was absent in some of the photoreceptor axon terminals, which were identified by the presence of punctate Cyt C immunostaining (Fig. 9B, arrows, inset, arrow). In 8-month-old DBA/2J retinas, there was a widespread loss of VGLUT1 immunostaining in the photoreceptor axon terminals. Horizontal cell processes extended to the vicinity of the mitochondria in the ONL, and these regions of the photoreceptor lacked VGLUT1 immunoreactivity (Fig. 9C, arrows). Some horizontal cell endings ramified in the ONL and were isolated from photoreceptor axon terminals and mitochondria (Fig. 9C, arrowheads). Horizontal cell endings in the rod spherules were not present (Fig. 9C, inset) and the rod spherules containing VGLUT1 immunoreactivity were reduced in size. All of these morphological changes were more prominent in regions of the outer retina overlying patches of the inner retina lacking RGCs (Fig. 9D, inset).

In 16-month-old DBA/2J retinas (Figs. 9E, 9F), the OPL was disrupted with a marked reduction of VGLUT1 immunoreactive axonal terminals and loss of calbindin immunoreactive horizontal cell processes (Fig. 9E, arrows, inset). In regions of the OPL that did not overlie the patches of inner retina with RGC loss, the giant mitochondria were displaced to the ONL, whereas in ONL regions overlying the patches lacking RGCs, the number of giant mitochondria decreased, likely due to the reduction of the number of photoreceptors. Furthermore, in OPL regions overlying the inner retina patches lacking RGCs, rod spherules had smaller appearance than those in the C57BL/6J control retinas and the horizontal cell endings, based on calbindin immunostaining and the giant mitochondria, based on Cyt C immunostaining were not observed (Fig. 9F, inset).

Discussion

Functional studies performed with glaucoma patients,[40,41] and on glaucoma experimental animal models[42] and genetic models[13,15,43] showed that the a- and b-waves of the ERG were diminished compared with normal, age-matched controls.

Findings from the present study also showed outer retina pathology in the DBA/2J model in addition to their well-established loss of RGCs and axons. Altered ERGs are also correlated with outer retinal damage in a model of acute ocular hypertension,[42] and recently, rod photoreceptor synaptic contacts have been reported to be reduced with aging.[18] The morphological changes described in this work could underlie the altered ERG responses observed in the DBA/2J mouse retina reported by other authors.[13,15]

Photoreceptor and ON bipolar cells[16,17] mainly mediate the a- and b-waves of the ERG response. In this study, we performed an exhaustive characterization of the outer retina using immunohistochemical techniques with cellular markers for photoreceptor, bipolar, and horizontal cells, before and after an increase in IOP in the DBA/2J mouse line. In general, IOP in this line begins to increase at approximately 6 months of age.[11,44] In the DBA/2J line, alterations in the ONL and OPL were first observed at 3 months of age, before the increase of IOP. At this age, there was a diminution of photoreceptor cell bodies and OPL thickness, as well as a reduction in the occurrence of both pre- and postsynaptic markers. The present study is in contrast to two earlier findings that the outer retina is unchanged in the DBA/2J mouse retina after the development of ocular pathology.[10,29]

In the DBA/2J retina at all ages, there are changes in the connectivity of photoreceptor cells and their postsynaptic contacts, shown by a reduction in their connections with bipolar cell dendrites and horizontal cell processes. In addition, we have found retraction of bipolar and horizontal cell processes and a disruption of the photoreceptor synaptic triad. Interestingly, in the 8- and 16-month-old DBA/2J retinas, some horizontal and bipolar cell processes were located in the ONL, suggesting their growth was concomitant with outer retinal degeneration; interestingly, at 3 months of age, bipolar and horizontal cell processes were shorter, suggesting a retraction of their processes. These results disagree with findings from Fuchs et al.[18] They described no alteration in horizontal and bipolar cells and attributed the thinning of the OPL to structural changes in rod synaptic ribbon but not cone photoreceptors.[18] We have carefully evaluated the pre- and postsynaptic elements of the synaptic contacts in the OPL showing the loss of bipolar and horizontal cell dendrites and axons.

The growth of bipolar cell dendrites into the overlying ONL is a common feature in animal models of photoreceptor degeneration, including rd mice,[45–47] the Royal College of Surgeons (RCS) rats,[48] and P23H rats.[27]

There are only a few functional and morphological studies of young DBA/2J mouse retinas; smaller amplitudes of the second harmonic component of the flicker responses are noted at 2 to 3 months old compared with those registered in wild-type animals, which could be due to the disruption of the synaptic triad in the photoreceptor terminals.[13] Furthermore, alterations in RIBEYE staining in rod photoreceptor ribbons were detected at 2 months old.[18] These findings are consistent with the idea that the Tyrp1 mutation that DBA/2J mice carry is expressed in the RPE,[49] which may indirectly affect photoreceptor cells, as the health of the RPE is essential for the integrity of photoreceptors and normal retinal function.[50] For instance, in the adult retina, mutations altering the function of RPE lead to photoreceptor death.[48,51]

With aging and IOP increased, the morphological changes in the OPL become quite prominent. In regions of the outer retina inside patches, cellular degeneration is accelerated compared with other retinal regions. Moreover, at 16 months of age, the photoreceptor triad is disrupted and apparently absent in most cases, and the horizontal cell plexus is absent. These morphological alterations in the OPL also have been described in an animal model of experimentally induced increase of IOP.[42]

Using double and triple immunostaining with markers for the synaptic ribbon, photoreceptor terminal, and for bipolar and horizontal cell processes, we studied the organization of the synaptic ribbon in the DBA/2J model. A decrease in photoreceptor ribbons with increased age was observed in the DBA/2J retina, based on the loss of Bassoon and CtBP2 immunoreactivity. Furthermore, we showed that although some photoreceptor axons expressed CtBP2, there was an absence of VGLUT1 immunoreactivity in the same terminals, suggesting that synaptic release of glutamate is greatly diminished or absent in the OPL,[52] which is essential for visual information transmission.[53] These findings, together with the decoupling between photoreceptor terminals, bipolar cell dendrites, and horizontal cell processes revealed by the loss of PKC and syntaxin 4 immunoreactivity, respectively, adjacent to synaptic ribbon markers is indicative of an impairment of the rod and cone synaptic structure.

Overall, these findings indicate a reduction in outer retinal signaling between photoreceptors, and bipolar cell dendrites and horizontal cell processes. This suggestion is consistent with a reduced ERG b-wave[54] in the Bassoon knockout mouse,

which is characterized by a severely disrupted photoreceptor triad.

There are several different possibilities to account for the outer retinal pathology we observed in the DBA/2J retina.

First, outer retina impairment might be related to mutations of RPE genes and not to elevated IOP, as the *Tyrp1* gene is expressed by the RPE, at least at the initial stages of outer retinal degeneration. Retinal pigment epithelium dysfunction is a well-established cellular mechanism for photoreceptor and outer retinal diseases. Royal College of Surgeons rats are a good example of a retinitis pigmentosa animal model carrying a mutation in an RPE gene.[55] Mutations in *Tyrp1* gene have been related to the etiology of human oculocutaneous albinism type 3. Moreover, mutations in this gene generate endoplasmic reticulum stress due to misfolded protein accumulation,[56] which could drive to RPE alterations. In addition, it has been shown that number of rod-photoreceptors is closely related to melanin levels in the RPE[57] and the fact that photoreceptors from albino animals are more susceptible to light damage[58,59] suggests the basis for outer retinal degeneration in DBA/2J mice.

Second, the increase of the IOP could result in two independent events: RGC and axonal damage that lead to RGC death, and photoreceptor cell damage that leads to outer retinal degeneration. This possibility cannot account for the changes in the outer retina that occur in young DBA/2J mice, before an increase of IOP.

Last, the mutations that the DBA/2J mice carry lead to ocular pathology typical of glaucoma before IOP increase, suggesting that this mouse glaucoma model is an IOP-independent glaucoma model. This suggestion is also based on findings that the DBA/2J model has two episodes of RGC loss[10]: one occurs before the increase of IOP and is mainly mediated by apoptosis, and the second occurs after an increase IOP and is mainly mediated by necrosis. These observations are consistent with the early alterations in the outer and inner retina during an IOP-independent component followed by a component with increased IOP.

Acknowledgments

Supported by grants from the Spanish Ministry of Economy and Competitivity-FEDER (BFU2012-36845), Instituto de Salud Carlos III (RETICS RD12/0034/0010), National Organization of Spanish Blind (ONCE1-13I), FUNDALUCE (Foundation for Fighting Blindness, Spain), National Institutes of Health EY04067 (NCB), National Institute of Diabetes and Digestive and Kidney Diseases P30 DK41301 (University of California Los Angeles Cure Center Core), and a Department of Veterans Affairs (VA) Merit Review (NCB). NCB is a VA Career Research Scientist.

Disclosure: **L. Fernández-Sánchez**, None; **L. Pérez de Sevilla Müller**, None; **N.C. Brecha**, None; **N. Cuenca**, None

References

1. Quigley HA. Ganglion cell death in glaucoma: pathology recapitulates ontogeny. *Aust N Z J Ophthalmol*. 1995;23:85–91.
2. Quigley HA. Neuronal death in glaucoma. *Prog Retin Eye Res*. 1999;18:39–57.
3. Pascolini D, Mariotti SP. Global estimates of visual impairment: 2010. *Br J Ophthalmol*. 2012;96:614–618.
4. Libby RT, Anderson MG, Pang I-H, et al. Inherited glaucoma in DBA/2J mice: pertinent disease features for studying the neurodegeneration. *Vis Neurosci*. 2005;22:637–648.
5. Schlamp CL, Li Y, Dietz JA, Janssen KT, Nickells RW. Progressive ganglion cell loss and optic nerve degeneration in DBA/2J mice is variable and asymmetric. *BMC Neurosci*. 2006;7:66.
6. Steele MR, Inman DM, Calkins DJ, Horner PJ, Vetter ML. Microarray analysis of retinal gene expression in the DBA/2J model of glaucoma. *Invest Ophthalmol Vis Sci*. 2006;47:977–985.
7. Niyadurupola N, Broadway DC. Pigment dispersion syndrome and pigmentary glaucoma-a major review. *Clin Experiment Ophthalmol*. 2008;36:868–882.
8. Chang B, Smith R. Interacting loci cause severe iris atrophy and glaucoma in DBA/2J mice. *Nat Genet*. 1999;21:405–409.
9. Anderson MG, Smith RS, Hawes NL, et al. Mutations in genes encoding melanosomal proteins cause pigmentary glaucoma in DBA/2J mice. *Nat Genet*. 2002;30:81–85.
10. Schuettauf F, Rejdak R, Walski M, et al. Retinal neurodegeneration in the DBA/2J mouse-a model for ocular hypertension. *Acta Neuropathol*. 2004;107:352–358.
11. John SW, Smith RS, Savinova OV, et al. Essential iris atrophy, pigment dispersion, and glaucoma in DBA/2J mice. *Invest Ophthalmol Vis Sci*. 1998;39:951–962.
12. Raymond ID, Pool AL, Vila A, Brecha NCA. Thy1-CFP DBA/2J mouse line with cyan fluorescent protein expression in retinal ganglion cells. *Vis Neurosci*. 2009;26:453–465.
13. Harazny J, Scholz M, Buder T, Lausen B, Kremers J. Electrophysiological deficits in the retina of the DBA/2J mouse. *Doc Ophthalmol*. 2009;119:181–197.
14. Barabas P, Huang W, Chen H, et al. Missing optomotor head-turning reflex in the DBA/2J mouse. *Invest Ophthalmol Vis Sci*. 2011;52:6766–6773.
15. Heiduschka P, Julien S, Schuettauf F, Schnichels S. Loss of retinal function in aged DBA/2J mice—new insights into retinal neurodegeneration. *Exp Eye Res*. 2010;91:779–783.
16. Brown K, Wiesel T. Localization of origins of electroretinogram components by intraretinal recording in the intact cat eye. *J Physiol*. 1961;158:257–280.
17. Tomita T. Electrical activity of vertebrate photoreceptors. *Nihon Seirigaku Zasshi*. 1970;32:567–568.
18. Fuchs M, Scholz M, Sendelbeck A, et al. Rod photoreceptor ribbon synapses in DBA/2J mice show progressive age-related structural changes. *PLoS One*. 2012;7:e44645.
19. Fernández-Sánchez L, Lax P, Pinilla I, Martín-Nieto J, Cuenca N. Tauroursodeoxycholic acid prevents retinal degeneration in transgenic P23H rats. *Invest Ophthalmol Vis Sci*. 2011;52:4998–5008.
20. Fernández-Sánchez L, Lax P, Esquiva G, Martín-Nieto J, Pinilla I, Cuenca N. Safranal, a saffron constituent, attenuates retinal degeneration in P23H rats. *PLoS One*. 2012;7:e43074.
21. Rodriguez-de la Rosa L, Fernandez-Sanchez L, Germain F, et al. Age-related functional and structural retinal modifications in the Igf1–/– null mouse. *Neurobiol Dis*. 2012;46:476–485.
22. Martinez-Navarrete G, Seiler MJ, Aramant RB, Fernandez-Sanchez L, Pinilla I, Cuenca N. Retinal degeneration in two lines of transgenic S334ter rats. *Exp Eye Res*. 2011;92:227–237.
23. Dowling JE, Chappell RL. Neural organization of the median ocellus of the dragonfly. II. Synaptic structure. *J Gen Physiol*. 1972;60:148–165.
24. Kolb H, Nelson R, Ahnelt P, Cuenca N. Cellular organization of the vertebrate retina. *Prog Brain Res*. 2001;131:3–26.
25. Linberg K, Cuenca N, Ahnelt P, Fisher S, Kolb H. Comparative anatomy of major retinal pathways in the eyes of nocturnal and diurnal mammals. *Prog Brain Res*. 2001;131:27–52.
26. Brandstätter JH, Fletcher EL, Garner CC, Gundelfinger ED, Wässle H. Differential expression of the presynaptic cytomatrix protein bassoon among ribbon synapses in the mammalian retina. *Eur J Neurosci*. 1999;11:3683–3693.
27. Cuenca N, Pinilla I, Sauvé Y, Lu B, Wang S, Lund RD. Regressive and reactive changes in the connectivity patterns of rod and

cone pathways of P23H transgenic rat retina. *Neuroscience*. 2004;127:301–317.

28. Martínez-Navarrete GC, Martín-Nieto J, Esteve-Rudd J, Angulo A, Cuenca N. Alpha synuclein gene expression profile in the retina of vertebrates. *Mol Vis*. 2007;13:949–961.
29. Jakobs TC, Libby RT, Ben Y, John SWM, Masland RH. Retinal ganglion cell degeneration is topological but not cell type specific in DBA/2J mice. *J Cell Biol*. 2005;171:313–325.
30. Peng Y-W, Senda T, Hao Y, Matsuno K, Wong F. Ectopic synaptogenesis during retinal degeneration in the royal college of surgeons rat. *Neuroscience*. 2003;119:813–820.
31. Ritchey ER, Bongini RE, Code KA, Zelinka C, Petersen-Jones S, Fischer AJ. The pattern of expression of guanine nucleotide-binding protein beta3 in the retina is conserved across vertebrate species. *Neuroscience*. 2010;169:1376–1391.
32. Gong J, Jellali A, Mutterer J, Sahel JA, Rendon A, Picaud S. Distribution of vesicular glutamate transporters in rat and human retina. *Brain Res*. 2006;1082:73–85.
33. Heidelberger R, Thoreson WB, Witkovsky P. Synaptic transmission at retinal ribbon synapses. *Prog Retin Eye Res*. 2005; 24:682–720.
34. tom Dieck S, Altrock WD, Kessels MM, et al. Molecular dissection of the photoreceptor ribbon synapse: physical interaction of Bassoon and RIBEYE is essential for the assembly of the ribbon complex. *J Cell Biol*. 2005;168:825–836.
35. Schmitz F, Konigstorfer A, Sudhoff TC. RIBEYE, a component of synaptic ribbons: a protein's journey through evolution provides insight into synaptic ribbon function. *Neuron*. 2000; 28:857–872.
36. Hirano A, Brandstatter J, Vila A, Brecha N. Robust syntaxin-4 immunoreactivity in mammalian horizontal cell processes. *Vis Neurosci*. 2007;24:489–502.
37. Medrano CJ, Fox DA. Oxygen consumption in the rat outer and inner retina: light- and pharmacologically-induced inhibition. *Exp Eye Res*. 1995;61:273–284.
38. Heidelberger R. Roles of ATP in depletion and replenishment of the releasable pool of synaptic vesicles. *J Neurophysiol*. 2002;88:98–106.
39. Johnson JE, Perkins GA, Giddabasappa A, et al. Spatiotemporal regulation of ATP and Ca2+ dynamics in vertebrate rod and cone ribbon synapses. *Mol Vis*. 2007;13:887–919.
40. Korth M, Nguyen NX, Horn F, Martus P. Scotopic threshold response and scotopic PII in glaucoma. *Invest Ophthalmol Vis Sci*. 1994;35:619–625.
41. Vaegan, Graham SL, Goldberg I, Buckland L, Hollows FC. Flash and pattern electroretinogram changes with optic atrophy and glaucoma. *Exp Eye Res*. 1995;60:697–706.
42. Cuenca N, Pinilla I, Fernández-Sánchez L, et al. Changes in the inner and outer retinal layers after acute increase of the intraocular pressure in adult albino Swiss mice. *Exp Eye Res*. 2010;91:273–285.
43. Bayer AU, Neuhardt T, May AC, et al. Retinal morphology and ERG response in the DBA/2NNia mouse model of angle-closure glaucoma. 2001;42:1258–1265.
44. Saleh M, Nagaraju M, Porciatti V. Longitudinal evaluation of retinal ganglion cell function and IOP in the DBA/2J mouse model of glaucoma. *Invest Ophthalmol Vis Sci*. 2007;48:4564–4572.
45. Rossi C, Strettoi E, Galli-Resta L. The spatial order of horizontal cells is not affected by massive alterations in the organization of other retinal cells. *J Neurosci*. 2003;23:9924–9928.
46. Strettoi E, Pignatelli V. Modifications of retinal neurons in a mouse model of retinitis pigmentosa. *Proc Natl Acad Sci U S A*. 2000;97:11020–11025.
47. Strettoi E, Pignatelli V, Rossi C, Porciatti V, Falsini B. Remodeling of second-order neurons in the retina of rd/rd mutant mice. *Vision Res*. 2003;43:867–877.
48. Cuenca N, Pinilla I, Sauve Y, Lund R. Early changes in synaptic connectivity following progressive photoreceptor degeneration in RCS rats. 2005;22:1057–1072.
49. Mori M, Metzger D, Garnier J-M, Chambon P, Mark M. Site-specific somatic mutagenesis in the retinal pigment epithelium. *Invest Ophthalmol Vis Sci*. 2002;43:1384–1388.
50. Raymond SM, Jackson IJ. The retinal pigmented epithelium is required for development and maintenance of the mouse neural retina. *Curr Biol*. 1995;5:1286–1295.
51. Pinilla I, Cuenca N, Sauvé Y, Wang S, Lund RD. Preservation of outer retina and its synaptic connectivity following subretinal injections of human RPE cells in the Royal College of Surgeons rat. *Exp Eye Res*. 2007;85:381–392.
52. Schuettauf F, Thaler S, Bolz S, et al. Alterations of amino acids and glutamate transport in the DBA/2J mouse retina; possible clues to degeneration. *Graefes Arch Clin Exp Ophthalmol*. 2007;245:1157–1168.
53. Johnson J, Fremeau RT, Duncan JL, et al. Vesicular glutamate transporter 1 is required for photoreceptor synaptic signaling but not for intrinsic visual functions. *J Neurosci*. 2007;27: 7245–7255.
54. Dick O, tom Dieck S, Altrock WD, et al. The presynaptic active zone protein bassoon is essential for photoreceptor ribbon synapse formation in the retina. *Neuron*. 2003;37:775–786.
55. D'Cruz PM, Yasumura D, Weir J, et al. Mutation of the receptor tyrosine kinase gene Mertk in the retinal dystrophic RCS rat. *Hum Mol Genet*. 2000;9:645–651.
56. Toyofuku K, Wada I, Valencia JC, Kushimoto T, Ferrans VJ, Hearing VJ. Oculocutaneous albinism types 1 and 3 are ER retention diseases: mutation of tyrosinase or Tyrp1 can affect the processing of both mutant and wild-type proteins. *FASEB J*. 2001;15:2149–2161.
57. Donatien P, Jeffery G. Correlation between rod photoreceptor numbers and levels of ocular pigmentation. *Invest Ophthalmol Vis Sci*. 2002;43:1198–1203.
58. Sanyal S, Zeilmaker GH. Retinal damage by constant light in chimaeric mice: implications for the protective role of melanin. *Exp Eye Res*. 1988;46:731–743.
59. Jansen HG, Sanyal S. Synaptic changes in the terminals of rod photoreceptors of albino mice after partial visual cell loss induced by brief exposure to constant light. *Cell Tissue Res*. 1987;250:43–52.
60. Barhoum R, Martínez-Navarrete G, Corrochano S, et al. Functional and structural modifications during retinal degeneration in the rd10 mouse. *Neuroscience*. 2008;155:698–713.
61. Rossé T, Olivier R, Monney L, et al. cl-2 prolongs cell survival after Bax-induced release of cytochrome c. *Nature*. 1998;391: 496–499.
62. Zhang H, Li S, Doan T, et al. Deletion of PrBP/delta impedes transport of GRK1 and PDE6 catalytic subunits to photoreceptor outer segments. *Proc Natl Acad Sci U S A*. 2007;104: 8857–8862.